A Systematic Investigation on Magnetism and Phase Stability of Cobalt

Fang-Guang Kuang, Xiao-Yu Kuang, and Shu-Ying Kang

Institute of Atomic and Molecular Physics, Sichuan University, Chengdu 610065, China

Reprint requests to X. Y. K.; E-mail: scu_kxy@163.com

Z. Naturforsch. **69a**, 254 – 262 (2014) / DOI: 10.5560/ZNA.2014-0024
Received January 15, 2014 / revised March 17, 2014 / published online May 21, 2014

Using the first-principles plan-wave pseudo-potential method, a systematic investigation on structural property, magnetism, and pressure-induced phase transitions of cobalt is carried out. Cobalt with four hcp (α), fcc (β), bcc (γ), and epsilon (ε) phases both in ferromagnetic (FM) and nonmagnetic (NM) states is considered. Issues of fitting equation of states in the energy volume data points containing magnetism are discussed. Our results reveal two stable phase transition points, namely, from FM β-phase to FM α-phase at -28.2 GPa and from FM α-phase to NM β-phase at 123.7 GPa, which are consistent with previous experimental predictions. The meta-stable magnetic transformation points from FM to NM state for α, β, and ε structures are 135.7 GPa, 84.0 GPa, and 168.7 GPa, respectively. Furthermore, both FM γ-phase and FM ε-phase undergo a meta-stable transformation to NM β-phase at 25.0 GPa and 42.3 GPa, respectively.

Key words: First-Principles; Magnetism; Phase Transition; Cobalt.

1. Introduction

The 3*d* metals magnetic transition studies are beneficial to a better understanding of the magnetism and structural properties of the Earth's interior. Among these elements, great efforts have been devoted to iron under high pressures both in experiments and theory, as it is the major constituent of the Earth's core [1, 2]. However, cobalt as the center of the 3*d* transition metal series was less studied, although works about cobalt at mega-bar pressure is crucial to the systematic understanding of the magnetic 3*d* elements.

As well known, metallic cobalt had four different crystal structures, including body-centered-cubic phase (bcc or γ), face-centered-cubic phase (fcc or β), hexagonal close-packed phase (hcp or α), and primitive cubic phase (epsilon or ε), which were refined by experimental studies [3 – 6]. A sketch view of these four structures is shown in Figure 1. The α-phase Co was most studied among these structures and often compared with bcc Fe. The reason is that the crystal structures of bcc Fe and α-phase Co are different from other nonmagnetic 3*d* transition metals. The difference originate in the spin polarized *d* band which can alter the *d* occupancy [7]. For the bcc Fe, its magnetism is rapidly suppressed and it will change into nonmagnetic (NM) hcp Fe at 10 GPa [8, 9]. By contrast, the magnetism of α-phase Co can hold in a wide range of abnormal pressures, and no phase transition is reported at room temperature up to 80 GPa [10 – 12]. So, α-phase Co with good magnetic stability seem to be atypical compared with bcc Fe and other transition metals. And the highest isotropic magnetic coercivity of the α-phase Co made it apply magnetic records. Controversially, resent research showed that the α-phase Co in the pressure range of 105 – 150 GPa will transform into a symmetrical low coercivity β-phase, the one which is useful for applications as a soft magnetic material [13]. The new discovery brings a stirring of interest in studying cobalt. Because it is only found that β-phase Co can exist above 420 °C and is quenched at room temperature as a meta-stable phase in the past. Moreover, Walmsley et al. [14] try to stabilize cobalt in a 'forced' bcc structure of polycrystalline modulated films of cobalt and chromium in view of iron stable bcc structure. Prinz also succeed in stabilizing bcc Co via epitaxial growth on GaAs [15]. A variety of experiments hereafter indicated that bcc Co is very similar to bcc Fe both electronically and magnetically. The ε-phase possess a more complex structure, which is reported by Dinega and Bawendi [16]. The synthesis of the ε-phase have been only possible by means of solution-phase chemistry processes. In the past few years, ε-phase Co has received great attentions because

of the fact that it seems to be a good precursor to obtain ε-phase nanoparticles for magnetic storage uses. As a soft magnetic material, its magnetic properties favor the formation of ordered films with applications in magnetic recording.

The physical characteristics of cobalt under high pressures have been great concern both in experiments and theory. Using a diamond-anvil cell and an imaging plate, Fujihisa and Takemura reported the bulk modulus and its pressure derivative as well as the axial ratio of α structure Co up to 79 GPa [17]. It was found that α-phase Co remained stable up to 79 GPa and the axial c/a ratio continuously decreased under pressure. With regard to stability of cobalt, Yoo et al. first discovered that there was a martensitic structural transition from α-Co to β-Co at $\sim$ 100 GPa by means of X-ray powder diffraction (XRPD) [13]. Since then, magnetism in β-phase Co has attracted great interest. Followed, large studies on cobalt under high pressures such as elasticity and vibrational properties were reported [18, 19]. However, to our knowledge, the systematic investigation on magnetism and phase stability of cobalt were few attentions by theoretical calculations. Yamamoto estimated that the transition pressure from α-phase to β-phase was 128.3 GPa by full-potential linearized augmented plane wave (FP-LAPW) method [20]. He obtained the same conclusion with Yoo et al. that the transformed β-Co is NM. Recently, based on density functional theory (DFT), a detailed study on the magnetic phase transformations of α-phase and β-phase of a cobalt crystal was derived [21]. However, only two structures were considered. There was no systematic work to investigate these four structures of the cobalt crystal.

In this paper, these four structures of single cobalt crystal in NM and FM states are investigated with different exchange correlation functionals based on first principles. This paper is organized as follows: after presenting the detail of calculations, we discuss the results of the equations of state, magnetic stability, and pressure-induced structural phase transitions. Conclusions are given in the final section.

2. Details of Calculations

Our first-principles calculations were carried out using the standard frozen-core projector augmented-wave [22] (PAW) method based on DFT as implemented in the Vienna ab initio simulation package [23] (VASP) code. The electronic exchange-correlation interactions were treated by the local density approximation (LDA) in the scheme of Ceperley and Alder [24] as parameterized by Perdew and Zunger [25], generalized gradient approximation (GGA) of Perdew-Wang (PW91) [26] and Perdew–Burke–Ernzerhof (PBE) [27]. Considered the rigor of calculations, we performed computations for both FM and NM states, allowing for a precise assessment of the influence of spin on physical properties. On the other hand, the Hubbard U correction was also taken into consideration. The Dudarev implementation with on-site Coulomb interaction $U = 2.8$ eV and on-site exchange interaction $J = 1.0$ eV to treat the localized $3d$ electronic states were chosen. The electronic wave functions were expanded in a plane-wave basis set with an energy cutoff of 500 eV. The k-space integrations were performed using $11 \times 11 \times 11$ Monkhorst–Pack meshes in the first Brillouin zone for β, γ, and ε structures, and the gamma-centered k-point mesh of $13 \times 13 \times 9$ for α structure. The tolerances self-consistent convergence of the total energy were tested within 10^{-5} eV/atom.

Considering the effect of pressure on the system, the geometrical parameters and the international positions of all phases at a number of fixed volumes were optimized. The total-energy versus volume data of all phases were obtained after carrying out the optimizations. A common practice was to fit the calculated total-energy versus volume $(E-V)$ data to an appropriate equation of state (EOS), and then obtain pressure by $p = -\partial E/\partial V$. In general, the widely utilized EOSs were the third-order Brich–Murnaghan (BM3) EOS [28] and the Vinet EOS [29]. In this work, two of these EOSs were used to fit the $E-V$ data. The BM3 EOS can be expressed as [30]

$$E(V) = -\frac{9}{16}B_0\left[\left(4-B_0'\right)\frac{V_0^3}{V^2} - (14-3B_0')\frac{V_0^{7/3}}{V^{4/3}} + \left(16-3B_0'\right)\frac{V_0^{5/3}}{V^{2/3}}\right] + E_0\,, \tag{1}$$

where V is the volume of the unit cell. The equilibrium volume (V_0) is found by minimizing the energy with respect to volume. The bulk modulus $B_0 = -V_0(\partial p/\partial V)_0$ is computed from the definition $B(V) = V(\partial^2 E/\partial V^2)$. Its first and second pressure derivative (B_0' and B_0'') are defined by $B_0' = (\partial B/\partial p)_{p=0}$ and $B_0'' = (\partial^2 B/\partial p^2)_{p=0}$, respectively. While the energies with volume of Vinet EOS is [29]

Table 1. Calculated equilibrium volume per unit cell V_0 (Å^3), bulk modulus B_0 (GPa), and its first pressure derivative B_0' of bcc (or γ) structure cobalt with different EOSs by different types of pseudo potential. The magnetic moments M (μ_B) and the cohesive energy E_{coh} (eV) are also listed in the table. Experimental data and previous calculations in the literature are provided for comparison.

States	Method	Type	EOS	V_0	B_0	B_0'	M	E_{coh}	Ref.
NM	PAW	PW91	BM3	10.56	232.9	4.72		5.01	
			Vinet	10.53	246.1	4.81		5.02	
		LDA	BM3	9.80	289.7	4.75		6.55	
			Vinet	9.81	303.7	4.68		6.57	
		PBE	BM3	10.57	231.5	4.72		5.19	
			Vinet	10.54	244.6	4.81		5.20	
		LSDA		10.66	269			6.50	[31]
FM	PAW	PW91	BM3	11.13	196.7	4.56	1.68	5.33	
			Vinet	11.08	207.0	4.72	1.67	5.34	
		LDA	BM3	10.19	248.0	4.60	1.57	6.74	
			Vinet	10.19	260.9	4.60	1.57	6.75	
		PBE	BM3	11.16	194.8	4.52	1.70	5.54	
			Vinet	11.11	204.9	4.72	1.69	5.54	
		PBE+U	BM3	11.23	171.9	4.96	1.92	4.78	
			Vinet	11.22	181.7	4.97	1.92	4.79	
		LMTO-LSDA		11.16	245		1.73	6.35	[31]
		Expt		11.29			1.41		[15]

Table 2. Calculated results for fcc (or β) structure.

States	Method	Type	EOS	V_0	B_0	B_0'	M	E_{coh}	Ref.
NM	PAW	PW91	BM3	10.32	251.5	4.87		5.24	
			Vinet	10.33	255.8	4.71		5.24	
		LDA	BM3	9.60	314.1	4.90		6.82	
			Vinet	9.62	313.5	4.58		6.82	
		PBE	BM3	10.33	249.9	4.86		5.42	
			Vinet	10.34	254.3	4.71		5.43	
		GGA		10.32	249	4.80			[21]
	LAPW	GGA		10.28	258	4.70			[19]
	PAW	GGA		10.35					[32]
	LSDA			10.54	264			6.61	[31]
	Exp			10.33	224	5.8			[13]
FM	PAW	PW91	BM3	10.96	198.7	4.26	1.60	5.42	
			Vinet	10.94	203.1	4.29	1.59	5.42	
		LDA	BM3	9.95	250.7	4.54	1.49	6.87	
			Vinet	9.96	257.0	4.44	1.49	6.88	
		PBE	BM3	10.96	197.2	4.38	1.62	5.61	
			Vinet	10.96	201.7	4.37	1.62	5.62	
		PBE+U	BM3	11.10	182.4	4.68	1.79	4.81	
			Vinet	11.10	183.6	4.70	1.79	4.81	
	LAPW	GGA		10.95	198	4.3			[19]
	LAPW	GGA		10.94	247				[18]
	PWSCF	GGA		10.97	214	3.2			[18]
		GGA		10.95	197	4.4			[21]
		GGA+U		11.16				3.79	[33]
	Exp			11.08	180	4			[15]
	LMTO-LSDA			11.03	235		1.64	6.36	[21]

$$E(V) = E_0 + \frac{9B_0V_0}{\xi^2}\left\{1 + \left[\xi(1-x) - 1\right] \cdot \exp\left[\xi(1-x)\right]\right\}. \quad (2)$$

E_0, V_0 is the zero pressure equilibrium energy and volume, respectively. And $x = (V/V_0)^{1/3}$ and $\xi = 3/2(B_0' - 1)$, B_0 is the bulk modulus and $B_0' = (\partial B/\partial p)_{p=0}$.

Table 3. Calculated results for hcp (or α) structure.

States	Method	Type	EOS	V_0	B_0	B_0'	M	E_{coh}	Ref.
NM	PAW	PW91	BM3	10.34	247.5	4.83		5.23	
			Vinet	10.35	259.3	4.75		5.24	
		LDA	BM3	9.61	309.0	4.85		6.80	
			Vinet	9.64	318.4	4.66		6.81	
		PBE	BM3	10.35	245.9	4.83		5.41	
			Vinet	10.35	257.8	4.75		5.42	
		GGA		10.35	248	4.8			[21]
	LAPW	GGA		10.31	256	4.7			[19]
	LMTO	LSDA		10.54	276			6.60	[31]
FM	PAW	PW91	BM3	10.86	203.0	4.58	1.59	5.41	
			Vinet	10.84	213.6	4.60	1.59	5.42	
		LDA	BM3	10.87	211.2	4.92	1.53	6.90	
			Vinet	10.89	207.8	4.52	1.54	6.89	
		PBE	BM3	10.91	200.6	4.56	1.59	5.62	
			Vinet	10.90	210.6	4.60	1.59	5.63	
		PBE+U	BM3	10.91	197.3	4.34	1.70	4.78	
			Vinet	10.90	197.5	4.48	1.70	4.78	
	LMTO-LSDA			11.03	240		1.63	6.39	[31]
	Expt			11.00	199	3.6			[15]
		GGA		10.93	206	4.3			
	LAPW	GGA		10.90	210	4.1			[19]
	WIEN2K-GGA			10.97	205				[18]
	PWSCF	GGA		11.02	189	4.8			[18]
	Exp						1.58		[34]

Table 4. Calculated results for complex cubic (or ε) structure.

States	Method	Type	EOS	V_0	B_0	B_0'	M	E_{coh}	Ref.
NM	PAW	PW91	BM3	10.58	242.0	4.79		5.14	
			Vinet	10.58	242.4	4.79		5.14	
		LDA	BM3	9.84	300.4	4.78		6.70	
			Vinet	9.84	300.9	4.79		6.70	
		PBE	BM3	10.59	240.2	4.78		5.32	
			Vinet	10.59	240.9	4.80		5.32	
FM		LDA	BM3	10.24	262.3	4.94	1.54	6.85	
			Vinet	10.24	262.7	4.95	1.54	6.86	
		PBE	BM3	11.13	202.5	4.79	1.64	5.59	
			Vinet	11.13	203.8	4.81	1.64	5.59	
		PBE+U	BM3	11.16	183.2	5.04	1.79	4.76	
			Vinet	11.16	184.1	5.10	1.79	4.76	
	PAW-PW91			11.11				5.45	[33]
	PAW-PW91+U			11.50				3.70	[33]
	Exp			11.33					[6]

3. Results and Discussions

3.1. Equations of State

In order to validate the parameters for further investigation, the exchange correlation functionals including LDA, PW91, and PBE are employed to optimize the four structures of cobalt within FM and NM states. The considered phases of cobalt as a function of volume are examined by calculating the energy versus volume ($E-V$) curves. Then, both the universality of Vinet EOS and the accuracy of BM3 EOS are used to fit the $E-V$ data.

The results of γ, β, α, and ε structures are listed in Tables 1, 2, 3, and 4, respectively. The contents of tables are the type of the magnetic states, the calculated method, and the type of EOSs. In detail, our results include the equilibrium volume V_0 (Å^3), the bulk modulus B_0 (in GPa), the bulk modulus' first pressure derivative B_0', the magnetic moment M (in μ_B), and

the cohesive energy E_{coh} (in eV) are summarized in tables. The cohesive energy is defined as the difference between the energy of an isolated atom and the energy of the same atom in the solid. Additionally, previous calculations [18, 19, 21, 31 – 33] and experimental data [6, 13, 15, 34] at room temperature in the literature are provided for comparison. Next, let us take our focus on Table 3, which displays the structural properties of the widely investigated α-phase. It is apparent that our results are in excellent agreement with the previous calculations. So our calculations are reliable in accuracy. Compared with experiments, several important features can be obtained:

(i) The LDA method slightly underestimates the equilibrium volume, but overestimates the bulk modulus and cohesive energy.
(ii) The results obtained by PBE method is more excellent than PW91 method.
(iii) Accurate structural properties by PBE+U method indicate that the electrons of cobalt exist stronger correlation effects.
(iv) The equilibrium volume in both EOS fittings is close, while the bulk modulus by BM3 EOS fitting is closer to experiments.

Tables 1, 2, and 3 can also give similar conclusions, so there is no need to present a detailed discussion. In summary, the PBE method with BM3 EOS fitting is most suitable for investigating structural properties of our system. Moreover, the stronger correlation effects of cobalt must be considered if the studies refer to the magnetic and electronic properties.

Shown in Tables 1 – 4, the cohesive energy in the FM state shows an interesting relationship. Namely, at the considered phases appear a relationship which is $E_{\gamma-\mathrm{coh}} < E_{\varepsilon-\mathrm{coh}} < E_{\beta-\mathrm{coh}} < E_{\alpha-\mathrm{coh}}$. It is suggested that the most stable structure at zero pressure is the FM α-phase, and then follows the FM β-phase. But for the NM state, the relationship of cohesive energy becomes $E_{\gamma-\mathrm{coh}} < E_{\varepsilon-\mathrm{coh}} < E_{\alpha-\mathrm{coh}} < E_{\beta-\mathrm{coh}}$. It is obviously that the β-phase turns into the most stable structure in the NM state. It should be point out that the relationships of cohesive energy can also be obtained by LDA and PW91 method. When the Hubbard U correction (PBE+U) is considered, the relationship of cohesive energy changes significantly. Compared with above conclusion of cohesive energy in FM state by PBE method, it is maybe the electronic correlation effects of the γ-phase that are stronger than other phases.

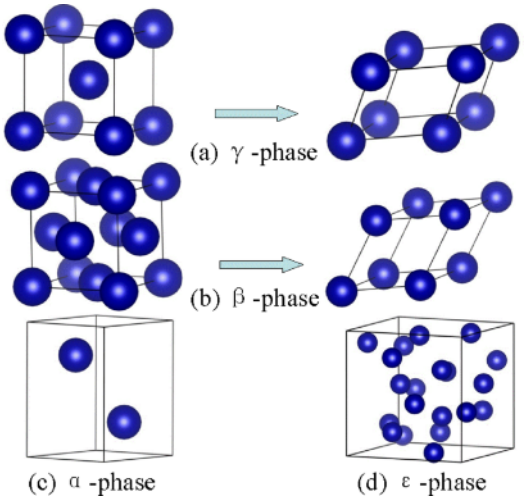

Fig. 1 (colour online). Sketch view of different bulk cobalt structures: (a) bcc or γ, (b) fcc or β, (c) hcp or α, and (d) complex cubic phase or ε.

So there is need to analyze the difference in magnetic moments between PBE method and PBE+U method.

3.2. Magnetic Stability

The magnetic moments of the ferromagnetic ground state of our studies are $1.70\mu_B$, $1.62\mu_B$, and $1.59\mu_B$ for bulk γ, β, and α-phase, respectively. The results of β and α-phase are in reasonable agreement with experimental values, i. e. $1.60\mu_B$ and $1.58\mu_B$ [34]. The calculated magnetic moments for the γ-phase ($1.70\mu_B$) agrees with other calculations [31] but it seems much larger than the measured value ($1.41\mu_B$) [15]. This disagreement may originate from defects in the sample, which is meta-stable and do not appear in the bulk phase diagram. It exists still no experiment on ε-phase, but our result does not appear exceptionally. All of these demonstrate that our calculations are credible. Additionally, as the Hubbard U correction is considered, the magnetic moment increases while the equilibrium volume almost not changes.

More in depth, the volume dependence of magnetic moments and the total energy of a unit cell are necessary to study. To elaborate on this problem, the magnetic moments and the energy difference between the FM and NM states as a function of volume of γ, β, and α structure are shown in Figures 2 and 3. It is noted that experimental and theoretical results are also displayed in these figures. Figure 1a displays the energy

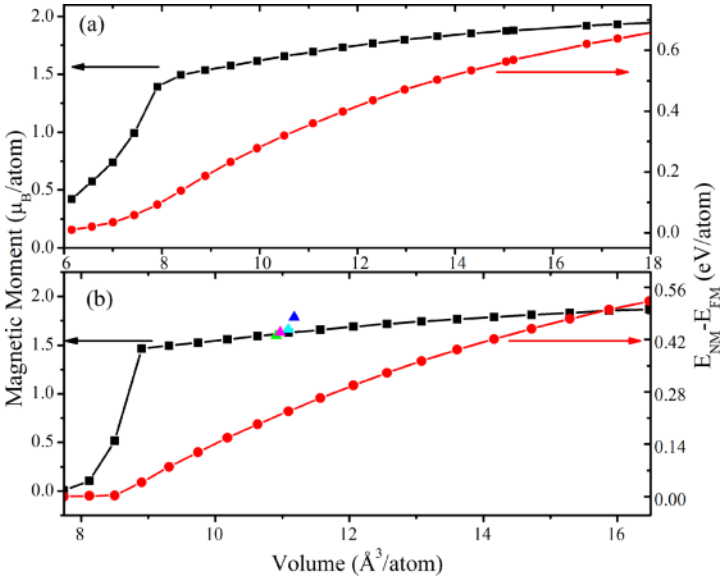

Fig. 2 (colour online). Magnetic moment and energy difference between the FM and NM states as a function of volume: (a) bcc or γ-phase; (b) fcc or β-phase. Filled triangles refer to experimental measurements of the magnetic moment of β-phase.

difference between the FM and NM states of γ-phase. It is observed that the energy difference goes to zero when the volume is less than 6 Å^3. So the magnetic moments do not contribute on the total energy in this case. It is a contradiction to the correlation theory, and it maybe because the pure γ structure of cobalt is unstable. Shown in Figure 1b, the FM β-phase still has magnetic moments even if the energy difference is zero. It is reflected that the FM β structure of cobalt maybe no longer presents the ferromagnetic state under high pressures. It also reveals that only from the energy difference it is difficult to determine the phase of β structure in FM state or NM state under high pressures. Shown in Figure 3, the energy difference between FM and NM states for alpha structure cobalt exists in all of the volumes. It means that the FM state of α structure is always more stable than the NM state. But the energy difference will be not obvious as the volume of the unit cell is less than 7 Å^3, which suggests there will be a meta-stable phase transformation. Moreover, the magnetic moments of the FM α-phase more slowly vanishes, reaching zero at about 7.3 Å^3. The magnetic moments of α-phase cobalt would completely vanish at a compression of $\sim 0.7V_0$, analogous to a pressure of $\sim$ 150 GPa. And it is consistent with previous X-ray magnetic circular dichroism (XMCD) results [35]. It is also observed that the magnetic moments of the FM α-phase is sustained at smaller volumes and goes to zero more gradually than the FM β-phase. In addition, compared with γ and β structures, the magnetic moments of the FM α structure have greater impact on the total energy. When the volume serious deviates from the equilibrium volume, the energy difference will approach a constant value. Further, the volume depen-

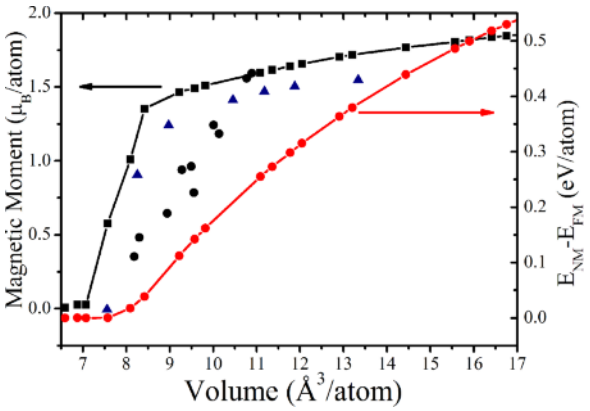

Fig. 3 (colour online). Magnetic moment of hcp or α-phase cobalt and energy difference between FM and NM states as a function of volume. Closed circles refer to experimental measurements of the magnetic moment of the α-phase at 298 K [35]. Filled triangles are the ferromagnetic moment for cobalt from [19] by LAPW calculations.

Table 5. Pressure of Cobalt phase transformations predicted from current first-principles calculations.

Transformation	Source	Pressure (GPa)
Stable		
FM β to FM α	Current work	−28.2
	[21]	−31
	Exp of [13]	~ -25
FM α to NM β	Current work	123.7
	[20]	128.3
	[21]	99
	Exp of [13]	~ 109
Meta-stable		
FM β to NM β	Current work	84.0
	[21]	77
FM α to NM α	Current work	135.7
	[21]	123
FM ε to NM ε	Current work	168.7
FM γ to NM β	Current work	25.0
FM ε to NM β	Current work	42.3

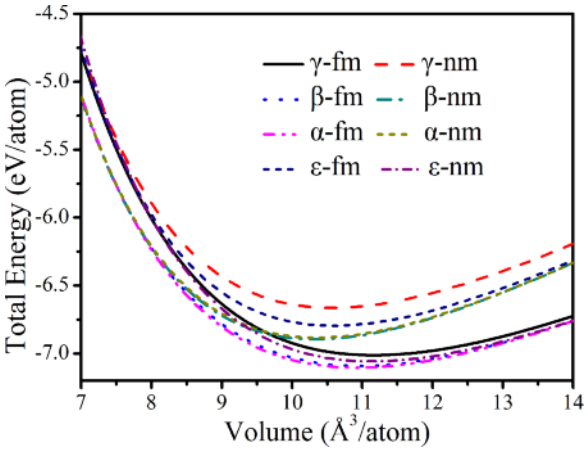

Fig. 4 (colour online). Calculated total energy as functions versus volume curves for different cobalt phases.

dence of magnetic moments for the ε structure displays complex changes.

3.3. Structural Phase Transitions

The calculated total energy as functions versus volume ($E-V$) curves for separate cobalt phases by PBE method are shown in Figure 4. In agreement with experiments and previous computations, the $E-V$ curves show that the FM α-phase is stable for a large volume range. It also shows that the FM α-phase has the lowest total energy of all phases while the NM γ-phase has the highest total energy of all the structures. In this case, it is unambiguously determined that the NM γ-phase is the most unstable. In order to more clearly observe the total energy difference of additional phases and compared them with the FM α-phase, the total energy versus volume for different cobalt phases with FM α-phase as the reference state is shown in Figure 5. It can also be predicted the possibility of a phase transformation from the figure. In detail, there will be some phase transformations appearing in FM β-phase, FM α-phase, and FM γ-phase under negative pressure. Taking note on high pressures, FM α-phase, FM β-phase, FM ε-phase, and NM β-phase may be also phase transformations.

Generally speaking, the Gibbs energy is the standard of determining the phase stability. The Gibbs energy of a unit cell expresses as $G = E + pV - TS$, where E is the total energy of the unit cell. It can be obtained directly from the first-principles quantum-mechanical calculations. p is the external pressure and V is the volume of the unit cell under the pressure. T and S are given in the temperature and the entropy. Consider the temperature is equal to 0 K in the first-principles calculations. The Gibbs energy at 0 K is equivalent to the enthalpy: $H = E + pV$, where $p = -\mathrm{d}E/\mathrm{d}V$. So a stable structure at a given pressure is one for which enthalpy has its lowest value, and thus the transition from one phase to another is given by a pressure at which the enthalpies for the two phases are equal in first-principle calculations. In detail, the function between the pressure and the enthalpy can be obtained by fitting the

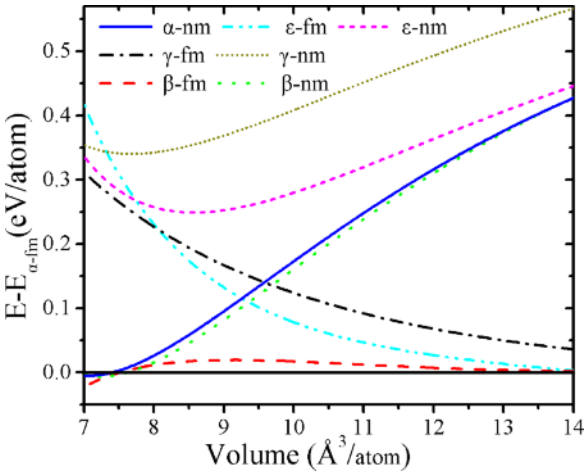

Fig. 5 (colour online). Total energy versus volume for different cobalt phases with FM α-phase as reference state.

$E-V$ data within BM3 EOS. Specifically, the enthalpy as a function of pressure, $H(p)$, is expressed by [30] $H(p) = E + (BV_0/B' - 1) \cdot \{[(B'/B) \cdot p + 1]^{1-1/B'} - 1\}$. In the equation, V_0, B, and B' are the equilibrium volume at zero-pressure, bulk modulus, and its first-order pressure derivative, respectively. On account of the four structures possess similar energetic stabilities and, hence, small temperatures or pressure variations give rise to changes in the crystal phase. Five phase transformations are predicted and summarized in Table 5. It should be point out that there is no phase transition between FM ε-phase and other phases, as same as the FM γ-phase.

As shown in Table 5, there are two stable structural transformations in these five phases at 0 K because they have the lowest Gibbs energies at the given pressure. Specifically, FM β-phase transforms into FM α-phase at -28.2 GPa and FM α-phase undergoes transition to NM β-phase at 123.7 GPa. These two phase transformations are in qualitative sensible agreement with the experimental cobalt $p-T$ phase diagram, which suggests both a high pressure transformation and a negative pressure transformation. The predicted 0 K high pressure transformation is in line with previous studies and the high pressure phase of β structure is the NM β-phase. The calculated phase transition point is also close to the extrapolation result of experiment at 0 K, i. e. $\sim$ 109 GPa [13]. Our result is also consistent with the earlier supposition of structural and theoretical considerations [13, 20, 35]. Concerning the prediction of a negative pressure transformation, due to most materials may no longer be corporeal in large values of negative pressure. The negative pressure can be understood as environment of high temperatures. In this way, we can obtain the extrapolation of the experimental β Curie transformation data to ~ -150 GPa, which is much less than the transformational pressure of -28.2 GPa.

The meta-stable magnetic transformations from FM to NM of α, β, and ε structures are 135.7, 84.0 GPa, and 168.7 GPa shown in Table 5, respectively. Above two predictions are consistent with experiments. It is observed that the α-phase retains a magnetic moment up to the structural transformation of 105 GPa at room temperature [13]. And the transformation from FM to NM for α structure cobalt is estimated to be around 150 GPa from the experimental slope of magnetic moment at room temperature [36]. Furthermore, measurements [13] indicate the high pressure β phase is the NM state, which is consistent with the current prediction that the magnetic moment goes to zero at a pressure lower than the transformation pressure from FM α-phase to NM β-phase. The magnetic transformation on ε-phase is reported for the first time, we hope the theoretical results will be confirmed by experiments. The meta-stable phase transformation at 25.0 GPa from FM γ to NM β is also predicated. Owing to γ-phase cobalt can only be a single-crystal film but not appear in the bulk phase, we cannot confirm the possibility of this phase transformation in the actual environment. Nevertheless, that the γ-phase cobalt can be stabilized under the condition of negative pressure is consistent with other theoretical predictions. Furthermore, the FM ε-phase also undergoes a meta-stable transformation to the NM β-phase at 42.3 GPa. All of above meta-stable transformations reveal that the NM β-phase will turn into a most stable structure at high pressures.

4. Conclusions

To study the equations of state, magnetic properties, and structural phase transformations of α, β, γ, and ε structures with ferromagnetic and nonmagnetic states of cobalt crystal, first-principles plane-wave calculations are performed within the density functional theory. Summary, combined with discussions of magnetic stability and results of enthalpy, we obtain several phase transitions as follows:

(i) There are two stable phase transitions, namely, the FM β-phase transforms into the FM α-phase at -28.2 GPa and the FM α-phase undergoes transformation to the NM β-phase at 123.7 GPa.

(ii) The meta-stable magnetic transformation from ferromagnetic to nonmagnetic for α, β, and γ structure is 135.7 GPa, 84.0 GPa, and 168.7 GPa, respectively.

(iii) The meta-stable transformation between the FM γ-phase and the NM β-phase occurs at 25.0 GPa, and the transformation from the FM ε-phase to the NM β-phase is at 42.3 GPa.

[1] S. K. Saxena, L. S. Dubrovinsky, P. Häggkvist, Y. Cerenius, G. Shen, and H. K. Mao, Science **269**, 1703 (1995).
[2] D. Andrault, G. Fiquet, M. Kunz, F. Visocekas, and D. Häusermann, Science **278**, 831 (1997).
[3] M. Ohtake, O. Yabuhara, J. Higuchi, and M. Futamoto, J. Appl. Phys. **109**, 07C105 (2011).
[4] V. F. Puntes, K. M. Krishnan, and A. P. Alivisatos, Science **291**, 2115 (2001).
[5] V. A. de la Peña O'shea, P. Ramírez de la Piscina, N. Homs, G. Aromí, and J. L. G. Fierro, Chem. Mater. **21**, 5637 (2009).
[6] S. Sun and C. B. Murry, J. Appl. Phys. **85**, 4325 (1999).
[7] R. E. Cohen, L. Stixrude, and E. Wasserman, Phys. Rev. B **56**, 8575 (1997).
[8] E. Huang, W. A. Bassett, and P. Tao, J. Geophys. Res. Solid Earth **92**, 8129 (1987).
[9] H. K. Mao, W. A. Bassett, and T. Takahashi, J. Appl. Phys. **38**, 272 (1967).
[10] C. S. Yoo, P. Söderlind, and H. Cynn, J. Phys. Condens. Matter. **10**, L311 (1998).
[11] M. Erbudak, E. Wetli, M. Hochstrasser, D. Pescia, and D. D. Vvedensky, Phys. Rev. Lett. **79**, 1893 (1997).
[12] D. Antonangeli, M. Krisch, G. Fiquet, D. L. Farber, C. M. Aracne, J. Badro, F. Occelli, and H. Requardt, Phys. Rev. Lett. **93**, 215505 (2004).
[13] C. S. Yoo, H. Cynn, P. Söderlind, and V. Iota, Phys. Rev. Lett. **84**, 4132 (2000).
[14] R. Walmsley, J. Thompson, D. Friedman, R. M. White, and T. H. Geballe, IEEE T. Magn. **19**, 1992 (1983).
[15] G. A. Prinz, Phys. Rev. Lett. **54**, 1051 (1985).
[16] D. P. Dinega and M. G. Bawendi, Angew. Chem. Int. Ed. Engl. **38**, 1788 (1999).
[17] H. Fujihisa and K. Takemura, Phys. Rev. B **54**, 5 (1996).
[18] P. Modak, A. K. Verma, R. S. Rao, B. K. Godwal, and R. Jeanloz, Phys. Rev. B **74**, 012103 (2006).
[19] G. Steinle-Neumann, Phys. Rev. B **77**, 104109 (2008).
[20] T. Yamamoto, Adv. Quantum. Chem. **42**, 199 (2003).
[21] J. E. Saal, S. L. Shang, Y. Wang, and Z. Liu, J. Phys. Condens. Matter. **22**, 096006 (2010).
[22] G. Kresse and D. Joubert, Phys. Rev. B **59**, 1758 (1993).
[23] G. Kresse and J. Furthmuller, Comp. Mater. Sci. **6**, 15 (1996).
[24] D. M. Ceperley and B. J. Alder, Phys. Rev. Lett. **45**, 566 (1980).
[25] J. P. Perdew and A. Zunger, Phys. Rev. B **23**, 5048 (1981).
[26] J. P. Perdew and Y. Wang, Phys. Rev. B **45**, 13244 (1992).
[27] J. P. Perdew, K. Burke, and M. Ernzerhof, Phys. Rev. Lett. **77**, 3865 (1996).
[28] F. Birch, Phys. Rev. **71**, 809 (1947).
[29] P. Vinet, J. H. Rose, J. Ferrante, and J. R. Smith, J. Phys. Condens. Matter. **1**, 1941 (1989).
[30] F. Brich, J. Geophys. Res. **83**, 1257 (1978).
[31] B. I. Min, T. Oguchi, and A. J. Freeman, Phys. Rev. B **33**, 7852 (1986).
[32] Y. S. Mohammed, Y. Yan, H. Wang, K. Li, and X. Du, J. Magn. Magn. Mater. **322**, 653 (2010).
[33] V. A. de la Peña O'shea, P. R. I. de Moreira, A. Roldán, and F. Illas, J. Chem. Phys. **133**, 024701 (2010).
[34] H. P. Meyers and W. Sucksmith, P. Roy. Soc. A **207**, 427 (1951).
[35] V. Iota, J. H. P. Klepeis, C. S. Yoo, J. Lang, D. Haskel, and G. Srajer, Appl. Phys. Lett. **90**, 042505 (2007).
[36] A. F. Goncharov, J. Crowhurst, and J. M. Zaug, Phys. Rev. Lett. **92**, 115502 (2004).